Journal of Mathematical Modeling
Vol. 13, No. 4, 2025, pp. 900-923. Research Article

JMM

Layer-resolving mesh method for convection-diffusion delay problems with boundary turning points

Yimesgen Mehari Kebede*, **Awoke Andargie Tiruneh, Endalew Getnet Tsega**

Department of Mathematics, College of Science, Bahir Dar University, Bahir Dar, Ethiopia
Email(s): yimesgen2004@gmail.com, awoke248@yahoo.com, endalebdumath2016@gmail.com

Abstract. This paper introduces a numerical scheme designed to solve time-delay singularly perturbed parabolic convection-diffusion problems with turning points. A small parameter induces boundary layers, making standard methods ineffective. To tackle these challenges, we developed a layer-resolving numerical scheme using the Crank-Nicolson method (time) and a central finite difference method on a Shishkin mesh (space). The stability and parameter-uniform convergence analysis show that the error decreases quadratically. Numerical results demonstrate higher accuracy than the existing approaches.

Keywords: Singularly perturbed, layer resolving mesh, parameter-uniform, turning points, central-difference
AMS Subject Classification 2010: 65M06, 65M12, 65M15.

1 Introduction

Singularly perturbed delay partial differential equations (SPDPDEs) involve a small positive parameter, ε, multiplying the highest-order derivative term and at least one delay argument. These equations are categorized into space shift problems and time delay problems, depending on whether the shift occurs in space or time. The parameter ε can create boundary layers in certain regions of the domain, while the delay introduces a memory effect, making the solution dependent on both current and past states. This dual nature of SPDPDEs makes them challenging to solve, as they combine the complexities of singular perturbations and delay effects.

The presence of ε in the highest-order derivative term often leads to the formation of boundary layers or interior layers, where the solution exhibits rapid variations. These layers require specialized numerical techniques to resolve accurately, as standard methods may fail to capture the sharp transitions. On the other hand, the delay term introduces a dependence on the solution's history, which can significantly influence the behavior of the system. For instance, in time delay problems, the solution at a given time depends on its values at previous times, while in space shift problems, the solution at a point depends

*Corresponding author
Received: 12 April 2025 / Revised: 3 July 2025 / Accepted: 11 July 2025
DOI: 10.22124/jmm.2025.30347.2724

on its values at other locations in the domain. The interplay between the singular perturbation and delay effects makes SPDPDEs particularly challenging to analyze and solve. The boundary layers caused by ε require high-resolution methods, while the delay terms necessitate the storage and efficient computation of past solution states. These challenges become even more complex when the solution to the differential equation includes additional behavior, known as turning points.

Singularly perturbed partial differential equations (SPPDEs) with turning points (degeneracies) are complex and challenging problems that continue to require further research, as they arise in the mathematical modeling of various physical phenomena. Among these, problems with interior turning points represent the one-dimensional case of stationary convection-diffusion equations with a dominant convective term and a velocity field that changes sign within the domain (e.g., in a catch basin). In contrast, boundary turning point problems occur in geophysical models [11] and in the analysis of thermal boundary layers in laminar flows [39].

Singular perturbation problems (SPPs) with time delays are used to model real-world processes where the current state depends on past history, such as incubation periods, gestation times, or transportation lags [37]. These models are also applied in the study of infectious disease dynamics, accounting for factors like primary infection, treatment effects, and immune responses. For instance, consider a polluted river where contaminants are transported by convection (flow), diffuse due to turbulence, and undergo biochemical degradation (reaction) with a time delay (e.g., due to microbial adaptation). The riverbed may feature multiple bends (turning points), where the flow velocity changes direction or vanishes, resulting in the formation of boundary and internal layers.

A classic example of SPPs with time lag is an equation from numerical control modeling furnace processing of metal sheets [2]:

$$\frac{\partial u_\varepsilon(x,t)}{\partial t} = \varepsilon \frac{\partial^2 u_\varepsilon(x,t)}{\partial x^2} + v(g(u_\varepsilon(x,t-\tau)))\frac{\partial u_\varepsilon(x,t)}{\partial x} + c[f(u_\varepsilon(x,t-\tau)) - u_\varepsilon(x,t)], \tag{1}$$

where the temperature distribution of the metal sheet is denoted by $u_\varepsilon(x,t)$. Also, the heat source and the velocity with which metal sheet is moving are denoted by f and v, respectively. Both f and v are dependent on the term $u_\varepsilon(x,t-\tau)$. A fixed delay τ occurs because the controlling device can only process information at a finite speed. The presence of slow and fast processes in singularly perturbed differential equations makes them more difficult to get approximate solution [24].

The standard finite difference operator applied on uniform mesh, fail to generate a suitable numerical solution for singularly perturbed differential equations because the solution exhibits narrow regions of very fast variation, such as boundary layers, shocks or turning points, for example, as $\varepsilon \to 0$. The analysis becomes more complicated when some coefficients or terms are zero or explode at some points in the domain. This drawback motivates the development of advanced numerical methods that account for the relationship between the singular perturbation parameter, the delay or shift parameter, and the degeneracy, while ensuring the order of convergence and error constant remain independent of these parameters.

Over the past decade, numerical studies of SPPDEs with turning points have garnered considerable attention, as evidenced by a growing body of research [1, 6, 13–15, 17, 20–23, 38, 40, 45]. However, the development of uniformly convergent numerical methods for SPDPDEs with multiple turning points remains a largely uncharted territory. While significant progress has been made in designing parameter-uniform methods for SPDPDEs in 1D and 2D without multiple turning points [3,5,7,9,10,18,25,26,28–36, 41–43], only two methods have been proposed for cases involving multiple turning points [37, 44].

These methods employ the implicit Euler scheme for time discretization on a uniform mesh, coupled with a hybrid scheme for spatial discretization on a Shishkin mesh, achieving first-order convergence before Richardson extrapolation method was applied. To achieve a more accurate and robust numerical method than the previously mentioned approaches, this study employs the Crank–Nicolson method for time discretization on uniform mesh and the central finite difference method for space discretization on Shishkin mesh to solve SPDPDEs with multiple boundary turning points. A common challenge in such problems is the occurrence of oscillations when approximating the spatial first derivative using central finite differences on a uniform mesh. However, studies [8, 12, 19] have shown that Shishkin meshes provide a stable and effective framework for mitigating these issues.

Notation: In this article, C is used to denote a generic positive constant that is independent of ε and the mesh parameters. All functions defined on the domain $\mathscr{W} = \ominus_x \times (0,T]$, with $\ominus_x = (0,1)$ and $T > 0$, are evaluated using the maximum norm:

$$||g||_{\overline{\mathscr{W}}} = \sup_{x\in\overline{\mathscr{W}}} |g(x)|, \text{ where } \overline{\mathscr{W}} = [0,1]\times[0,T].$$

The boundary of the domain is $\partial\mathscr{W} = \overline{\mathscr{W}} \setminus \mathscr{W} = \Gamma_l \cup \Gamma_b \cup \Gamma_r$, where

$$\Big\{\Gamma_l = \{x=0 \mid 0 \le t \le T\},\ \ \Gamma_b = [0,1]\times[-\tau,0],\ \ \Gamma_r = \{x=1 \mid 0 \le t \le T\}.$$

2 Properties of continuous problem

In this article, we considered the following singularly perturbed parabolic convection-diffusion time-delay partial differential equations with Dirichlet boundary conditions:

$$\begin{cases} \mathscr{K}_\varepsilon u(x,t) = F(x,t), & (x,t)\in\mathscr{W}, \\ u(x,t) = \phi_b(x,t), & (x,t)\in\Gamma_b, \\ u(0,t) = \phi_l(t), \quad u(1,t) = \phi_r(t), & t\in(0,T], \end{cases} \tag{2}$$

where

$$\begin{cases} \mathscr{K}_\varepsilon u(x,t) \equiv (\varepsilon u_{xx} + a u_x - bu - u_t)(x,t), \\ F(x,t) = f(x,t) + c(x,t)u(x,t-\tau), \\ a(x,t) = a_0(x,t)x^p, \quad p\ge 1, \\ a_0(x,t)\ge\beta>0, \quad b(x,t)\ge\alpha>0, \quad c(x,t)\ge\gamma>0 \quad \text{on} \quad \overline{\mathscr{W}}, \end{cases} \tag{3}$$

for the functions $a(x,t)$, $b(x,t)$,$c(x,t)$ and $f(x,t)$ on $\overline{\mathscr{W}}$ and ϕ_l, ϕ_r, and ϕ_b on $\partial\mathscr{W}$, which are assumed to be smooth and bounded. Also, $0<\varepsilon\ll 1$ and $\tau>0$ are the singular perturbation and delay parameters, respectively.

For $p>1$, problem (2) is called a multiple boundary turning point problem. The characteristic curves of problem (2), when setting $\varepsilon=0$, are tangent to the left boundary Γ_l, leading to the formation of a boundary layer of width $\mathscr{O}(\sqrt{\varepsilon})$ in its neighbourhood [15].

Let $\phi_b(x,0)\in C^2[0,1]$ and ϕ_l, $\phi_r\in C^1[0,T]$. We impose the compatibility conditions

$$\phi_b(0,0) = \phi_l(0), \quad \phi_b(1,0) = \phi_r(1), \tag{4}$$

and

$$\begin{cases} \varepsilon \frac{\partial^2 \phi_b(0,0)}{\partial x^2} + a(0,0)\frac{\partial \phi_b(0,0)}{\partial x} - b(0,0)\phi_b(0,0) - \frac{\partial \phi_l(0)}{\partial t} = f(0,0) + c(0,0)\phi_b(0,-\tau), \\ \varepsilon \frac{\partial^2 \phi_b(1,0)}{\partial x^2} + a(1,0)\frac{\partial \phi_b(1,0)}{\partial x} - b(1,0)\phi_b(1,0) - \frac{\partial \phi_r(1)}{\partial t} = f(1,0) + c(1,0)\phi_b(1,-\tau), \end{cases} \tag{5}$$

to ensure that the data matches at the corners $(0,0)$, $(0,\tau)$, $(1,-\tau)$, and $(1,0)$.

The existence and uniqueness of the solution to problem (2) are assumed under the conditions that the solution is Hölder continuous and satisfies the compatibility conditions (4) and (5) [44]. These assumptions ensure that there exists a constant C such that, for all $(x,t) \in \bar{\mathscr{W}}$,

$$|u(x,t) - \phi_b(x,0)| \leq Ct. \tag{6}$$

Lemma 1. *The bound on the solution $u(x,t)$ of the continuous problem (2) is given by*

$$|u(x,t)| \leq C.$$

Proof. From equation (6), we have

$$|u(x,t)| - |\phi_b(x,0)| \leq |u(x,t) - \phi_b(x,0)| \leq Ct,$$

which implies that

$$|u(x,t)| \leq Ct + |\phi_b(x,0)|, \ \forall (x,t) \in \overline{\mathscr{W}}.$$

For $t \in [0,1]$, and since $\phi_b(x,0)$ is bounded, it follows that

$$|u(x,t)| \leq C.$$

□

Lemma 2. ***(The continuous minimum principle)*** *Let $\theta(x,t)$ be a sufficiently smooth function defined on $\mathscr{W}$ which satisfies $\theta(x,t) \geq 0, \forall (x,t) \in \partial\mathscr{W}$ and $\mathscr{K}_\varepsilon \theta(x,t) \leq 0, \ \forall (x,t) \in \mathscr{W}$. Then $\theta(x,t) \geq 0, \ \forall (x,t) \in \overline{\mathscr{W}}$.*

Proof. Interested reader can see the proof in [15]. □

Lemma 3. ***(Stability estimate)*** *Suppose $u(x,t)$ be the solution of (2). Then it satisfies*

$$||u(x,t)||_{\bar{\mathscr{W}}} \leq ||u(x,t)||_{\partial\mathscr{W}} + \frac{T}{\beta}||F(x,t)||_{\overline{\mathscr{W}}}.$$

Proof. One can see the proof in [15]. □

Theorem 1. *The solution u(x,t) and its partial derivatives satisfy the bound*

$$\left|\frac{\partial^{i+j}}{\partial x^i \partial t^j} u(x,t)\right| \leq C(1 + \varepsilon^{-i/2} exp(-x\sqrt{\frac{\beta}{\varepsilon}})), \ \ (x,t) \in \overline{\mathscr{W}},$$

where i and j are non-negative integers such that $0 \leq i + 3j \leq 4$.

Proof. For a fixed $i=0$ and on the boundaries $x=0$ and $x=1$ of $\overline{\ominus}$, we have $u=0$ and consequently $u_t=0$. On the boundary $t=0$, the condition $u=0$ implies that $u_x=0$ and $u_{xx}=0$. It then follows from (2) that

$$u_t(x,0)=F(x,0).$$

For $t\in(-\tau,0)$, we have

$$u_t=\lim_{l\to 0}\frac{u(x,t-\tau+l)-u(x,t-\tau)}{l}=0.$$

Thus, by choosing K_1 sufficiently large, we ensure that $|u_t(x,t)|\le K_1$ on $\partial\mathscr{W}$.

Using the assumption of Ng-Stynes in [27] for $a(x,t)$ in the domain $\overline{\mathscr{W}}$ and adopting the technique in [32], we express the differential operator $\mathscr{K}_\varepsilon$ defined in (2) as

$$\mathscr{K}_\varepsilon u(x,t)\equiv\varepsilon u_{xx}+(au)_x-(a_x+b)u-u_t.$$

Applying this operator to u_t yields

$$\begin{aligned}\mathscr{K}_\varepsilon u_t(x,t)&=\big(\varepsilon u_{txx}+(au_t)_x-(a_x+b)u_t-u_{tt}\big)(x,t)\quad as\quad a=a(x)\\&=\big(\varepsilon u_{txx}+au_{tx}-bu_t-u_{tt}\big)(x,t)\\&=\big(\varepsilon u_{xx}+au_x-bu-u_t\big)_t(x,t)+b_tu\\&=f_t(x,t)+c_t(x,t)u(x,t-\tau)+c(x,t)u_t(x,t-\tau)+b_tu.\end{aligned}\tag{7}$$

First, consider the case where $u(x,t-\tau)$ is a known function, which occurs when $t\in(0,\tau)$. Substituting the initial condition into (7), we obtain

$$\mathscr{K}_\varepsilon u_t(x,t)=f_t+b_tu.$$

Since f is sufficiently smooth, Lemmas 1 and 2 yield

$$|(\mathscr{K}_\varepsilon)\,u_t(x,t)|\le K_2,\quad (x,t)\in(0,1)\times(0,\tau),$$

and thus $|u_t|\le C$.

Next, we extend the analysis to the domain $(x,t)\in(0,1)\times(0,2\tau)$. For $t\in(\tau,2\tau)$, equation (7) becomes

$$\mathscr{K}_\varepsilon u_t(x,t)=f_t+c_tu(x,t-\tau)+cu_t(x,t-\tau)+b_tu.$$

Given that $|u_t|\le C$ on $(x,t)\in(0,1)\times(0,\tau)$, we have

$$|\mathscr{K}_\varepsilon u_t(x,t)|\le C\quad\text{for}\quad(x,t)\in(0,1)\times(\tau,2\tau).$$

Therefore, applying the minimum principle over the domain $(x,t)\in(0,1)\times(0,2\tau)$, we conclude that $|u_t|\le C$. By repeating this argument, we can establish the required bound over the entire domain $\overline{\mathscr{W}}$.

To bound the derivatives of the solution in the spatial domain, consider the cases for a fixed $j=0$. In the DPDE (2), the delay influences only the time variable t and has no impact on the spatial variable x. For $i=0$, from Lemma 1 we have $|u|\le C$. For $i=1$, by using arguments in [16], construct the neighbourhood of $I=(0,\sqrt{\varepsilon}),\ \forall r\in I$. By the mean value theorem, there exists some $r^*\in I$ such that

$$u_x(r^*)=\frac{u(\sqrt{\varepsilon})-u(0)}{\sqrt{\varepsilon}}.\tag{8}$$

This implies

$$|u_x(r^*)| = \varepsilon^{-1/2}|u(\sqrt{\varepsilon}) - u(0)| \leq C\varepsilon^{-1/2}\|u\|. \tag{9}$$

Rewriting Eq. (2) as

$$\mathscr{K}_\varepsilon u(x,t) \equiv \varepsilon u_{xx} + (au)_x - (a_x + b)u - u_t = F, \tag{10}$$

we obtain

$$\varepsilon u_{xx} + (au)_x = F + (a_x + b)u + u_t. \tag{11}$$

Integrating from r^* to r yields

$$\int_{r^*}^{r} (\varepsilon u_{xx} + (au)_x)\, dx = \int_{r^*}^{r} (F + (a_x + b)u + u_t)\, dx, \tag{12}$$

which gives

$$(\varepsilon u_x + au)|_{r^*}^{r} \leq C \int_{r^*}^{r} (\|F\| + \|u\| + \|u_t\|)\, dx \leq C\varepsilon^{1/2}. \tag{13}$$

Thus

$$\varepsilon u_x(r,t) + a(r,t)u(r,t) \leq \varepsilon u_x(r^*,t) + a(r^*,t)u(r^*,t) + C\varepsilon^{1/2}. \tag{14}$$

For $r \in (0, \sqrt{\varepsilon})$, we have $|a(r,t)| = |a_0(r,t)r^k| \leq C\varepsilon^{k/2}$ $(k = 1,2,3,\ldots)$. Using (9), we obtain

$$\begin{aligned}
|u_x(r,t)| &\leq |a(r^*,t)u(r^*,t)|/\varepsilon + |a(r,t)u(r,t)|/\varepsilon + C\varepsilon^{-1/2} \\
&\leq C_1\varepsilon^{-1/2} + C_2\varepsilon^{k/2-1} + C_3\varepsilon^{k/2-1} + C\varepsilon^{-1/2} \\
&\leq C_4\varepsilon^{-1/2} \leq C\left(1 + \varepsilon^{-1/2}\exp\left(-x\sqrt{\beta/\varepsilon}\right)\right).
\end{aligned}$$

For $i = 1$, the proof is complete. The required bounds for higher-order derivatives $(i = 2,3,4)$ follow similarly. □

To get the $\varepsilon-$uniform error estimate, one requires some stronger bound on the solution's derivatives. For this,we decompose the solution $u(x,t)$ into two parts: $u(x,t) = v(x,t) + w(x,t)$, where $v(x,t)$ is the regular component and $w(x,t)$ is singular component satisfying the following:

$$\begin{aligned}
\mathscr{K}_\varepsilon v(x,t) &= f(x,t) + c(x,t)u(x,t-\tau), && \text{on } \mathscr{W}, \\
v(x,t) &= v_0 + \varepsilon v_1 + \varepsilon^2 v_2, && \text{on } \Gamma_l, \\
v(x,t) &= u(x,t), && \text{on } \Gamma_b \cup \Gamma_r,
\end{aligned} \tag{15}$$

$$\begin{aligned}
\mathscr{K}_\varepsilon w(x,t) &= c(x,t)u(x,t-\tau), && \text{on } \mathscr{W}, \\
w(x,t) &= u(x,t) - v(x,t), && \text{on } \Gamma_l, \\
w(x,t) &= 0, && \text{on } \Gamma_b \cup \Gamma_r.
\end{aligned} \tag{16}$$

The following theorem establishes bounds for the derivatives of both the regular and singular components.

Theorem 2. *The regular and singular components, along with their derivatives, satisfy the following bounds:*

$$\left|\frac{\partial^{i+j}}{\partial x^i \partial t^j} v(x,t)\right| \leq C(1+\varepsilon^{3-i/2}), \left|\frac{\partial^{i+j}}{\partial x^i \partial t^j} w(x,t)\right| \leq C(\varepsilon^{-i/2} exp(-x\sqrt{\frac{\beta}{\varepsilon}})), \ \ (x,t) \in \overline{\mathscr{W}},$$

where i and j are non-negative integers such that $0 \leq i+3j \leq 4$.

Proof. The proof follows a similar approach to that in [1,4,37]. □

.

3 Formulation of the numerical scheme

We employed uniform mesh in the temporal direction and piece-wise uniform shishkin-type mesh in the spatial direction to generate a good approximate solution on the entire domain.

3.1 Temporal discretization

For $\varepsilon < \tau$, the Taylor series expansion cannot be applied to the term involving the delay parameter $u(x,t-\tau)$ in problem (2), as the point $t-\tau$ does not align with the mesh points after discretization. Consequently, we partitioned the time domain as follows:

$$\begin{aligned} \mathscr{W}_t^M &= \left\{ 0 = t_0 < t_1 < \cdots < t_k = \tau < \cdots < t_{M-1} < t_M = T \right\}, \\ \mathscr{W}_\tau^s &= \left\{ -\tau = t_{-k} < t_{-k+1} < \cdots < t_{-1} < t_0 = 0 \right\}, \end{aligned} \tag{17}$$

where M and s are the number of mesh elements in $[0,T]$ and $[-\tau,0]$, respectively, such that the uniform step size $\Delta t = \frac{T}{M} = \frac{\tau}{s}$ for each interval.

To discretize the time variable of (2), the Crank-Nicolson scheme is used. Eq.(2) at a time level $t_{j+1/2}$ can be written as

$$\begin{cases} \varepsilon U_{xx}^{j+1/2}(x) + a^{j+1/2}(x) U_x^{j+1/2}(x) - b^{j+1/2}(x) U^{j+1/2}(x) & \\ \qquad -D_t^- U^{j+1}(x) = F^{j+1/2}(x), & x \in \Omega_x,\ 0 \leq j \leq M-1, \\ U^{j+1}(0) = \phi_l(t_{j+1}), \quad U^{j+1}(1) = \phi_r(t_{j+1}), & 0 \leq j \leq M-1, \\ U^{-j}(x) = \phi_b(x, -t_j), & j = 0,1,2,\dots,s, \quad x \in \overline{\ominus}_x \end{cases} \tag{18}$$

where

$$D_t^- u^{j+1}(x) = \frac{U^{j+1}(x) - U^j(x)}{\Delta t}, U^{j+1/2}(x) = \frac{U^{j+1}(x) + U^j(x)}{2}, \quad F^{j+1/2}(x) = \frac{F^{j+1}(x) + F^j(x)}{2},$$

and $U^j(x)$ is an approximate solution of $u(x,t_j)$ at j^{th} time level.

The time semi-discretized problem (18) can be rewritten as

$$\begin{cases} \hat{\mathscr{K}}_\varepsilon U^{j+1}(x) = R^{j+1}(x), & x \in (0,1), \\ U^{j+1}(0) = \phi_l(t_{j+1}), & \\ U^{j+1}(1) = \phi_r(t_{j+1}), & 0 \le j \le M-1, \\ U^{-j}(x) = \phi_b(x,-t_j), & j = 0,1,2,...,s, \quad x \in \overline{\ominus}_x \end{cases} \tag{19}$$

where

$$\begin{cases} \hat{\mathscr{K}}_\varepsilon U^{j+1}(x) = \frac{\varepsilon}{2}(U_{xx})^{j+1} + \frac{a^{j+1}(x)}{2}(U_x)^{j+1} - \frac{q^{j+1}(x)}{2}(U(x))^{j+1}, \\ R^{j+1}(x) = F^{j+1/2}(x) - \frac{\varepsilon}{2}(U_{xx})^j - \frac{a^j(x)}{2}(U_x)^j + \frac{d^j(x)}{2}(U(x))^j, \\ q^{j+1}(x) = b^{j+1}(x) + \frac{2}{\Delta t}, \quad d^j(x) = b^j(x) - \frac{2}{\Delta t}, \end{cases}$$

and

$$F^j(x) = \begin{cases} f^j(x) + c^j(x)\phi_b(x, t_j - \tau), & j = 0,1,2,...,s, x \in \ominus_x, \\ f^j(x) + c^j(x)U^{j-s}(x), & j = s+1, s+2, ..., M-1, x \in \ominus_x. \end{cases}$$

The semi-discrete operator $\hat{\mathscr{K}}_\varepsilon$ satisfies the following minimum principle.

Lemma 4. ***(Minimum principle for temporal discretization)*** *Suppose $\theta^{j+1}(x)$ is a smooth function satisfying $\theta^{j+1}(0) \ge 0$, $\theta^{j+1}(1) \ge 0$ and $\hat{\mathscr{K}}_\varepsilon \theta^{j+1}(x) \le 0$ for all $x \in \ominus_x$. Then $\theta^{j+1}(x) \ge 0$ for all $x \in \overline{\ominus}_x$ and $j = 0,1,2,\ldots,M-1$.*

Proof. Let $\ell \in \ominus_x$ be such that $\theta^{j+1}(\ell) = \min_{x \in \ominus_x} \theta^{j+1}(x) < 0$. This implies that $(\theta^{j+1}(\ell))' = 0$ and $(\theta^{j+1}(\ell))'' \ge 0$. Then, we have

$$\hat{\mathscr{K}}_\varepsilon \theta^{j+1}(\ell) = \frac{\varepsilon}{2}(\theta^{j+1}(\ell))'' + \frac{a^{j+1}(x)}{2}(\theta^{j+1}(\ell))' - \frac{q^{j+1}(x)}{2}\theta^{j+1}(\ell) > 0.$$

Since

$$q^{j+1}(\ell) = b^{j+1}(\ell) + \frac{2}{k} \ge \beta + \frac{2}{k} > 0,$$

this contradicts the assumption that

$$\hat{\mathscr{K}}_\varepsilon \theta^{j+1}(x) \le 0.$$

Therefore, we conclude that

$$\theta^{j+1}(x) \ge 0 \text{ on } \overline{\mathscr{W}}.$$

$\square$

Lemma 5. *If $U^{j+1}(0) \ge 0$ and $U^{j+1}(1) \ge 0$, then*

$$\left|U^{j+1}(x)\right| \le \max\{U^{j+1}(0), U^{j+1}(1)\} + \max_{x \in \ominus_x} \frac{|\hat{\mathscr{K}}_\varepsilon U^{j+1}(x)|}{\beta}.$$

Proof. The proof is similar to the proof in [15]. $\square$

The local error of the time semi-discretization method (19) is given by $e_{j+1} \equiv u(x,t_{j+1}) - U^{j+1}(x)$, where $U^{j+1}(x)$ is the solution obtained after one step by taking the exact value $u(x,t_j)$ instead of $U^j(x)$ as the starting data.

Concretely, we have

$$\hat{\mathscr{K}}_\varepsilon U^{j+1}(x) \equiv \frac{\varepsilon}{2}(U_{xx})^{j+1} + \frac{a^{j+1}(x)}{2}(U_x)^{j+1} - \frac{q^{j+1}(x)}{2}(U(x))^{j+1} = R(x,t_{j+1}), \tag{20}$$

subject to the initial and boundary conditions

$$\begin{aligned} &U^{j+1}(0) = \phi_l(t_{j+1}), \quad U^{j+1}(1) = \phi_r(t_{j+1}), \quad 0 \le j \le M-1, \\ &U^{-j}(x) = \phi_b(x,-t_j), \quad j = 0,1,2,...,s, \quad x \in \overline{\ominus}_x, \end{aligned}$$

where

$$R^{j+1}(x) = F^{j+1/2}(x) - \frac{\varepsilon}{2}(U_{xx})^j - \frac{a^j(x)}{2}(U_x)^j + \frac{d^j(x)}{2}(U(x))^j.$$

Theorem 3. *Suppose that*

$$\left|\frac{\partial^i u}{\partial t^i}\right| \le C, \ \ (x,t) \in \overline{\mathscr{W}} \ \ for \ \ 0 \le i \le 2.$$

The local truncation error at $(j+1)^{th}$ time step is given by $||e_{j+1}|| \le C(\Delta t)^3$.

Proof. Using Taylor series expansion, we have

$$u(x,t_{j+1}) = u(x,t_{j+1/2}) + \frac{\Delta t}{2}u_t(x,t_{j+1/2}) + \frac{1}{2!}(\frac{\Delta t}{2})^2 u_{tt} + O(\Delta t)^3. \tag{21}$$

$$u(x,t_j) = u(x,t_{j+1/2}) - \frac{\Delta t}{2}u_t(x,t_{j+1/2}) + \frac{1}{2!}(\frac{\Delta t}{2})^2 u_{tt} + O(\Delta t)^3. \tag{22}$$

Subtracting (22) from (21), we obtain

$$\begin{aligned} \frac{u(x,t_{j+1}) - u(x,t_j)}{\Delta t} &= u_t(x,t_{j+1/2}) + O(\Delta t^2) \\ &= \varepsilon u_{xx}(x,t_{j+1/2}) + a(x,t_{j+1/2})u_x(x,t_{j+1/2}) \\ &\quad - b(x,t_{j+1/2})u(x,t_{j+1/2}) - F(x,t_{j+1/2}) + O(\Delta t^2), \end{aligned}$$

where $u(x,t_{j+1/2}) = \dfrac{u(x,t_{j+1}) + u(x,t_j)}{2} + O(\Delta t^2)$.

Further simplification yields

$$\hat{\mathscr{K}}_\varepsilon u(x,t_{j+1}) \equiv \frac{\varepsilon}{2}u_{xx}(x,t_{j+1}) + \frac{a(x,t_{j+1})}{2}u_x(x,t_{j+1}) - \frac{q(x,t_{j+1})}{2}u(x,t_{j+1}) = R(x,t_{j+1}) + O((\Delta t)^3). \tag{23}$$

From Eq. (20) and Eq. (23) the local truncation error satisfies

$$\begin{aligned} \hat{\mathscr{K}}_\varepsilon e_{j+1} =& O((\Delta t)^3), \\ e_{j+1}(0) =& e_{j+1}(1) = 0. \end{aligned} \tag{24}$$

It can be seen that $||e_{j+1}|| \le C(\Delta t)^3$. □

The local error estimate of each time step contributes to the global error in the temporal semi-discretization which is denoted by E_j.

Theorem 4. *The global truncation error for temporal discretization up to j^{th} time level is given by*

$$||E_j|| \leq C(\Delta t)^2, \quad \forall j \leq \frac{T}{\Delta t}.$$

Proof. Using the local error estimate up to j^{th} time step, we obtain the global error estimate at j^{th} time step as follow:

$$\begin{aligned} ||E_j|| =& ||\sum_{i=1}^{j} e_i||, \quad j \leq \frac{T}{\Delta t} \\ =& ||e_1|| + ||e_2|| + ||e_3|| + \cdots + ||e_j|| \\ \leq& C_1(j)(\Delta t)^3 \quad \text{(using Theorem 3)} \\ \leq& C_1 T(\Delta t)^2 \text{ as } \; j.\Delta t \leq T \\ \leq& C(\Delta t)^2, \;\; C = C_1 T. \end{aligned}$$

□

3.2 Spatial discretization

In this section, we outline the piecewise-uniform Shishkin mesh for discretizing the spatial domain and investigate the behavior of the difference scheme applied to discretize problem (2).

Owing to the presence of a boundary layer near $x = 0$ in problem (2), the mesh must be denser in the neighbourhood of $x = 0$. To construct the piecewise-uniform mesh, the domain $[0,1]$ is divided into two sub-intervals:

$$[0,1] = [0,\sigma] \cup (\sigma,1].$$

Each of these sub-intervals is then subdivided into $N/2$ equal parts, and the resulting spatial grids are denoted by

$$\bar{\ominus}^N = \{0 = x_0, x_1, \ldots, x_{N/2} = \sigma, \ldots, x_N = 1\},$$

where

$$x_i = \begin{cases} i\frac{2\sigma}{N}, & i = 0(1)\frac{N}{2}, \\ \sigma + (i - \frac{N}{2})\frac{2(1-\sigma)}{N}, & i = (\frac{N}{2}+1)(1)N, \end{cases}$$

and $N \geq 4$ be positive even integers.

The transition point σ, which separates the coarse and fine regions of the mesh, is determined by taking

$$\sigma = \min\{\frac{1}{2}, \sigma_0\sqrt{\varepsilon}\ln N\}, \text{where } \sigma_0 = \frac{1}{\sqrt{\beta}}. \tag{25}$$

Based on the definition of x_i, the spatial step sizes are for $i = 0,1,2,\ldots,N$ are defined as:

$$h_i = x_{i+1} - x_i = \begin{cases} h = \frac{2}{N}\sigma, & \text{if } \; i = 0(1)\frac{N}{2}, \\ H = \frac{2}{N}(1-\sigma), & \text{if } \; i = (\frac{N}{2}+1)(1)N, \end{cases}$$

where h and H represent the mesh widths in the intervals $[0,\sigma]$ and $(\sigma,1]$, respectively.
From these expressions, it follows that

$$N^{-1} \le H \le 2N^{-1}, \quad h = \frac{2\sigma_0\sqrt{\varepsilon}\ln N}{N}.$$

A uniform mesh can be achieved by setting $\sigma = \frac{1}{2}$.

In analyzing the error, we use $\sqrt{\varepsilon} \le CN^{-1}$ and $\sigma = \frac{2\sqrt{\varepsilon}}{\sqrt{\beta}}\ln N$, otherwise one can proceed with classical way. As $\varepsilon \to 0$, it is widely recognized that second-order central difference methods for approximating first-order derivatives in a differential equation result in an unstable numerical solution on a uniform mesh. However, studies in [12], [19] and [8] have shown that employing a Shishkin mesh ensures stability.

Thus, the full discretization on $W^{N,M}$ is of the form

$$\begin{cases} \hat{\mathscr{K}}_\varepsilon^N U_i^{j+1} \equiv \frac{\varepsilon}{2}\delta_x^2 U_i^{j+1} + \frac{a_i^{j+1}}{2} D_x^0 U_i^{j+1} - \frac{q_i^{j+1}}{2} U_i^{j+1} = R_i^{j+1}, & i \in \{1,\ldots,N-1\}, \\ U_0^{j+1} = \phi_l(t_{j+1}), & j \in \{0,\ldots,M-1\}, \\ U_N^{j+1} = \phi_r(t_{j+1}), & \\ U^{-j}(x) = \phi_b(x,-t_j), & j = 0,1,2,...,s, \quad x \in \overline{\ominus}_x, \end{cases} \tag{26}$$

where

$$\begin{cases} R_i^{j+1} = F_i^{j+1/2} - \frac{\varepsilon}{2}\delta_x^2 U_i^j - \frac{a_i^j}{2} D_x^0 U_i^j + \frac{d_i^j}{2} U_i^j, \\ q_i^{j+1} = b_i^{j+1} + \frac{2}{\Delta t}, \\ d_i^j = b_i^j - \frac{2}{\Delta t}, \end{cases}$$

$$F_i^j = \begin{cases} f_i^j + c_i^j \phi_b(x_i, t_j - \tau), & j = 0,1,2,...,s, \ i = 1,2,3,...,N-1, \\ f^j(x) + c^j(x) U^{j-s}(x), & j = s+1, s+2, ..., M-1, \ i = 1,2,3,...,N-1, \end{cases}$$

and the difference operators are defined by

$$\begin{cases} \delta_x^2 U_i^j = \dfrac{2(D^+ - D^-)}{\hat{h}} U_i^j, \\ D_x^0 U_i^j = \dfrac{U_{i+1}^j - U_{i-1}^j}{\hat{h}}, \end{cases} \quad \text{and} \quad \begin{cases} D_x^+ U_i^j = \dfrac{U_{i+1}^j - U_i^j}{h_{i+1}}, \\ D_x^- U_i^j = \dfrac{U_i^j - U_{i-1}^j}{h_i}, \\ \hat{h}_i = h_i + h_{i+1}. \end{cases}$$

The discrete scheme (26) can be written as

$$\hat{\mathscr{K}}_\varepsilon^N U_i^{j+1} \equiv r_i^- U_{i-1}^{j+1} + r_i^c U_i^{j+1} + r_i^+ U_{i+1}^{j+1} = y_i^- U_{i-1}^j + y_i^c U_i^j + y_i^+ U_{i+1}^j + H_i^{j+1/2} \tag{27}$$

with the discrete boundary and initial conditions

$$\begin{cases} U_0^{j+1} = \phi_l(t_{j+1}), U_N^{j+1} = \phi_r(t_{j+1}), & 0 \le j < M, \\ U^{-j}(x) = \phi_b(x,-t_j), & i \in \{1,\ldots,N-1\} \text{ and } j \in \{-s,\ldots,-1,0\}, \end{cases} \tag{28}$$

where the coefficients are given by

$$\begin{cases} r_i^- = \dfrac{2\varepsilon}{\hat{h}_i h_i} - \dfrac{a_i^{j+1}}{\hat{h}_i}, \\ r_i^c = -\dfrac{2\varepsilon}{h_i h_{i+1}} - (b_i^{j+1} + \frac{2}{\Delta t}), \\ r_i^+ = \dfrac{2\varepsilon}{\hat{h}_i h_{i+1}} + \dfrac{a_i^{j+1}}{\hat{h}_i}, \end{cases} \quad \text{and} \quad \begin{cases} y_i^- = -\dfrac{2\varepsilon}{\hat{h}_i h_i} + \dfrac{a_i^j}{\hat{h}_i}, \\ y_i^c = \dfrac{2\varepsilon}{h_i h_{i+1}} + b_i^j - \frac{2}{\Delta t}, \\ y_i^+ = -\dfrac{2\varepsilon}{\hat{h}_i h_{i+1}} - \dfrac{a_i^j}{\hat{h}_i}. \end{cases}$$

and the function that contains the delay parameter is

$$H_i^{j+1/2} = \begin{cases} f_i^{j+1/2} + c_i^{j+1/2}\phi_b(x_i, t_{j+1/2} - \tau), & j = 0,1,2,\ldots,s, \quad i = 1,2,\ldots,N-1, \\ f_i^{j+1/2} + c_i^{j+1/2} U_i^{j+1/2-s}, & j = s+1, s+2, \ldots, M-1, \quad i = 1,2,\ldots,N-1. \end{cases}$$

The coefficient matrix in Eq. (27) together with conditions (28) gives $(N-1)\times(N-1)$ tri-diagonal system of equations with unknowns $U_1, U_2, \ldots, U_{N-1}$ which can be solved using any tri-diagonal solvers such as Thomas Algorithm.

4 Convergence analysis

In this section, we first analyze the stability of the proposed scheme, followed by its consistency. Finally, we establish the convergence analysis through error estimation.

Lemma 6. *Assume that*

$$4\tau_0^2 \|a\|_\infty < \frac{N_0}{(\ln N_0)^2} \quad \textit{for} \quad N \geq N_0 \geq 8.$$

Then, we have

$$\begin{cases} r_i^- > 0, \quad r_i^+ > 0, \quad \textit{for } 1 \leq i \leq N, \\ |r_i^-| + |r_i^+| \leq |r_i^c|, \quad \textit{for } 1 \leq i \leq N. \end{cases}$$

Proof. It is clear that $r_i^+ > 0$. For r_i^-, we have

$$\begin{aligned} r_i^- &= \left(\frac{2\varepsilon}{\hat{h}_i h_i} - \frac{a_i^{j+1}}{\hat{h}_i}\right) \geq \left(\frac{2\varepsilon}{\hat{h}_i h_i} - \frac{\|a\|_\infty}{\hat{h}_i}\right) = \frac{1}{\hat{h}_i}\left(\frac{2\varepsilon}{h_i} - \|a\|_\infty\right) \\ &\geq \frac{N}{4\tau_0^2}\left(\frac{N}{\ln^2 N} - \|a\|_\infty 4\tau_0^2\right). \end{aligned}$$

Since for $N \geq N_0 \geq 8$,

$$\frac{N}{\ln^2 N} - \frac{N_0}{\ln^2 N_0} \geq 0,$$

it follows that $r_i^- > 0$.

Next,

$$
\begin{aligned}
|r_i^-|+|r_i^+| &= \left|\frac{2\varepsilon}{h_i\hat{h}_i}-\frac{a_i^{j+1}}{\hat{h}_i}\right|+\left|\frac{2\varepsilon}{h_{i+1}\hat{h}_i}+\frac{a_i^{j+1}}{\hat{h}_i}\right| \\
&= \frac{2\varepsilon}{h_i\hat{h}_i}-\frac{a_i^{j+1}}{\hat{h}_i}+\frac{2\varepsilon}{h_{i+1}\hat{h}_i}+\frac{a_i^{j+1}}{\hat{h}_i} \quad (\text{since } r_i^-, r_i^+ > 0) \\
&= \frac{2\varepsilon}{h_ih_{i+1}} \quad (\text{using } \hat{h}_i = h_i + h_{i+1}).
\end{aligned}
$$

We also have

$$|r_i^c| = \left|-\frac{2\varepsilon}{h_ih_{i+1}}-\left(b_i^{j+1}+\frac{2}{\Delta t}\right)\right| = \frac{2\varepsilon}{h_ih_{i+1}}+b_i^{j+1}+\frac{2}{\Delta t}.$$

Hence, $|r_i^-|+|r_i^+| < |r_i^c|$ for $1 < i < N$.

On the left boundary where $a(0,t) = 0$, we have

$$r_0^- = \frac{2\varepsilon}{\hat{h}_0h_0} > 0,$$

and

$$|r_0^c|-|r_0^+| = \left(\frac{\varepsilon}{h^2}+b_0^{j+1}+\frac{2}{\Delta t}\right)-\left(\frac{\varepsilon}{h^2}+\frac{a_0^{j+1}}{2h}\right) \geq b_0^{j+1}+\frac{2}{\Delta t} \geq \alpha+\frac{2}{\Delta t} > 0.$$

Similarly

$$|r_0^c|-|r_0^-| \geq b_0^{j+1}+\frac{2}{\Delta t} > 0.$$

On the right boundary, from $\varepsilon \leq \frac{1}{4\sigma_0^2\ln^2 N}$ and $H \leq 2N^{-1}$, we have

$$r_N^- = \frac{2\varepsilon}{H^2}-\frac{a_N^{j+1}}{H} \leq \frac{1}{H}\left(\frac{N}{2\sigma_0^2\ln^2 N}-\beta x_N^p\right).$$

Since $x_N^p \leq 1$ and $\sigma_0^2 = 1/\beta$,

$$r_N^- \leq \beta\left(\frac{N}{2\ln^2 N}-1\right) > 0 \quad \text{for} \quad N \geq 8.$$

For the right boundary conditions, we have

$$|r_N^c|-|r_N^+| \geq b_N^{j+1}+\frac{2}{\Delta t}-\frac{a_N^{j+1}}{2H} \geq \alpha+\frac{2}{\Delta t}-\frac{\|a\|_\infty}{2H} > 0,$$

and

$$|r_N^c|-|r_N^-| \geq b_N^{j+1}+\frac{2}{\Delta t}+\frac{a_N^{j+1}}{2H} > 0,$$

since $H = \Delta t$ in the coarse mesh region.

Thus, we conclude

$$|r_i^-|+|r_i^+| < |r_i^c| \quad \text{for} \quad 1 \leq i \leq N.$$

These show that the tri-diagonal matrix associated with (27) at each time level is M Matrix for $4\tau_0^2\|a\|_\infty < \frac{N_0}{(\ln N_0)^2}$ for $N \geq N_0 \geq 8$. Hence, the operator $\hat{\mathscr{K}}_\varepsilon^N$ in (27) satisfies the following discrete minimum principle for $4\tau_0^2\|a\|_\infty < \frac{N_0}{(\ln N_0)^2}$ for $N \geq N_0 \geq 8$. □

Lemma 7. ***(Discrete minimum principle)*** *Assume that* $U_0^{j+1} \geq 0, U_N^{j+1} \geq 0$ *and* $\hat{\mathscr{K}}_\varepsilon^N U_i^{j+1} \leq 0$, *for* $1 \leq i \leq N-1$. *Then* $U_i^{j+1} \geq 0 \quad$ *for* $\quad 1 \leq i \leq N$ *and* $1 \leq j < M$.

Lemma 8. *Assume that* $U^{j+1}(x_0) = U^{j+1}(x_N) = 0$. *Then, for* $h_i a_i^{j+1} \leq 2\varepsilon$ *we have the bound*

$$\left|U^{j+1}(x_i)\right| \leq \max_{x_i \in \ominus^N} |\hat{\mathscr{K}}_\varepsilon^N U^{j+1}(x_i)|, \;\; x_i \in \ominus_x.$$

To prove $\varepsilon-$uniform error estimates on singular components, the following barrier function are constructed:

$$\varphi_i^n(\mu) = \begin{cases} \prod_{k=1}^i \left(1 + \frac{\mu h_k}{\sqrt{\varepsilon}}\right)^{-1}, & 1 \leq i \leq N, \\ 1, & i = 0, \end{cases}$$

where $\mu = \sqrt{\beta}$ is a constant. Also

$$\begin{cases} \varphi_{i-1}^n(\mu) = \left(1 + \frac{\mu h_i}{\sqrt{\varepsilon}}\right)^{-1} \varphi_i^n(\mu), & 1 \leq i \leq N, \\ \varphi_{i+1}^n(\mu) = \left(1 + \frac{\mu h_{i+1}}{\sqrt{\varepsilon}}\right)^{-1} \varphi_i^n(\mu), & 1 \leq i \leq N-1. \end{cases}$$

Lemma 9. *The barrier function* $\varphi_i^n(\mu)$ *satisfies the following inequalities:*

$$\hat{\mathscr{K}}_\varepsilon^N \varphi_i^n(\mu) \leq -\frac{C}{\sqrt{\varepsilon}} \varphi_i^n(\mu) \quad \text{for} \quad 1 \leq i \leq N.$$

Proof. One can refer the proof in [37]. □

Lemma 10. *The mesh function* $\varphi_i^n(\mu)$ *satisfies the following inequality:*

$$e^{-\mu x_i/\sqrt{\varepsilon}} \leq \prod_{k=1}^{i} \left(1 + \frac{\mu h_k}{\sqrt{\varepsilon}}\right)^{-1} = \varphi_i^n(\mu), \quad \text{for all} \quad 0 \leq i \leq N,$$

and on Shishkin mesh, mesh function also satisfies the following inequality:

$$\prod_{k=1}^{i} \left(1 + \frac{\mu h_k}{\sqrt{\varepsilon}}\right)^{-1} \leq \begin{cases} CN^{-4i/N}, & 0 < i \leq \frac{N}{2}, \\ CN^{-2}, & \frac{N}{2} \leq i < N. \end{cases}$$

Theorem 5. *Let* $u_i(t)$ *and* $U_i(t)$ *be the solutions of the continuous and discrete problem, respectively. Then, the truncation error of the proposed scheme satisfy the following bounds:*

$$\sup_{0<\varepsilon\leq 1} |u_i(t) - U_i(t)| \leq CN^{-2} \ln^2 N \quad \text{for } i = 0, 1, \ldots, N,$$

where C *is a constant independent of* ε *and the mesh parameter* N.

Proof. We prove this theorem by decomposing the numerical solution U_i^N in (27) into regular and singular components, similar to the continuous problem, as:

$$U_i^j = V_i^j + W_i^j \quad \text{on the domain } \mathscr{W}^{N,M}.$$

Therefore, the pointwise error of the discrete solution at each mesh point (x_i, t_j) is decomposed as:

$$(u-U)_i^j = (v-V)_i^j + (w-W)_i^j. \tag{29}$$

We now estimate the error separately for the regular and singular components.

First, for the regular component:

$$\hat{\mathscr{K}}_\varepsilon^N (v-V)_i^j \le C\left[h_i(h_i+h_{i+1})(\varepsilon|v_{xxxx}|+|v_{xxx}|)\right].$$

For $\sigma = \frac{2\sqrt{\varepsilon}}{\sqrt{\beta}}\ln N$, the mesh is piecewise uniform, with spacing $h_i = \frac{2\sigma}{N}$ in the interval $(0,\sigma)$, *and* $h_i = \frac{2(1-\sigma)}{N}$ in the interval $(\sigma,1)$. Hence,

$$\hat{\mathscr{K}}_\varepsilon^N (v-V)_i^j \le \begin{cases} C\left[N^{-2}\sigma^2(\varepsilon|v_{xxxx}|+|v_{xxx}|)\right] & \text{on } (0,\sigma), \\ C\left[(N^{-1}(1-\sigma))^2(\varepsilon|v_{xxxx}|+|v_{xxx}|)\right] & \text{on } [\sigma,1). \end{cases} \tag{30}$$

Since $\sigma = \frac{2\sqrt{\varepsilon}}{\sqrt{\beta}}\ln N < \frac{1}{2}$, it follows that $1-\sigma \le C$. Using the bounds of the regular component (Theorem 2), we obtain

$$\hat{\mathscr{K}}_\varepsilon^N (v-V)_i^j \le CN^{-2} \quad \text{for } 1 \le i \le N. \tag{31}$$

Applying Lemma 8, we get $|v-V| \le CN^{-2}$ for $1 \le i \le N$.

Next, we estimate the truncation error for the singular component.

First, consider the outer layer region $[\sigma,1]$. In this region, both w and W are small. Using the triangle inequality and Theorem 2, we have

$$\begin{aligned} |(w-W)(x_i,t_j)| &\le |w(x_i,t_j)| + |W(x_i,t_j)| \le C\exp\left(-\frac{\sqrt{\beta}}{\sqrt{\varepsilon}}x_i\right) + C\prod_{k=i+1}^{N}\left(1+\frac{\sqrt{\beta}h_k}{\sqrt{\varepsilon}}\right)^{-1} \\ &\le C\prod_{k=1}^{i}\left(1+\frac{\sqrt{\beta}h_k}{\sqrt{\varepsilon}}\right)^{-1} + C\prod_{k=i+1}^{N}\left(1+\frac{\sqrt{\beta}h_k}{\sqrt{\varepsilon}}\right)^{-1} = C\prod_{k=1}^{N}\left(1+\frac{\sqrt{\beta}h_k}{\sqrt{\varepsilon}}\right)^{-1}. \end{aligned}$$

Using Lemma 10, the error bound in the outer region is given by

$$|(w-W)(x_i,t_j)| \le CN^{-2}, \quad (x_i,t_j) \in [\sigma,1]\times(0,T].$$

For the inner layer region $(x_i,t_j) \in [0,\sigma]\times(0,T]$, the truncation error becomes

$$\begin{aligned} \hat{\mathscr{K}}_\varepsilon^N (w-W)(x_i,t_j) &\le Ch_i\left[\int_{x_{i-1}}^{x_{i+1}}(\varepsilon|w_{xxxx}|+|w_{xxx}|)\,dx\right] \le C\frac{h_i}{\varepsilon^{3/2}}\left[\int_{x_{i-1}}^{x_{i+1}}\exp\left(-\sqrt{\frac{\beta}{\varepsilon}}x\right)dx\right] \\ &\le C\frac{h_i}{\sqrt{\beta}\varepsilon}\left[\exp\left(-\sqrt{\frac{\beta}{\varepsilon}}x_{i+1}\right) - \exp\left(-\sqrt{\frac{\beta}{\varepsilon}}x_{i-1}\right)\right] \\ &= C\frac{h_i}{\sqrt{\beta}\varepsilon}\left[\exp\left(-\sqrt{\frac{\beta}{\varepsilon}}x_i\right)\left\{\exp\left(\sqrt{\frac{\beta}{\varepsilon}}h\right) - \exp\left(-\sqrt{\frac{\beta}{\varepsilon}}h\right)\right\}\right] \\ &= C\frac{h_i}{\sqrt{\beta}\varepsilon}\left[\exp\left(-\sqrt{\frac{\beta}{\varepsilon}}x_i\right)\sinh\left(\sqrt{\frac{\beta}{\varepsilon}}h\right)\right]. \end{aligned}$$

Using the assumption in Lemma 6, we have $\sqrt{\frac{\beta}{\varepsilon}}h \leq 2$. Since $\sinh \nu \leq C\nu$ for $0 \leq \nu \leq 2$, it follows that

$$\sinh\left(\sqrt{\frac{\beta}{\varepsilon}}h\right) \leq \sqrt{\frac{\beta}{\varepsilon}}h.$$

Therefore, the above expression becomes

$$\hat{\mathscr{K}}_\varepsilon^N (w-W)_i^j \leq C\frac{h^2}{\varepsilon^{3/2}}\exp\left(-\sqrt{\frac{\beta}{\varepsilon}}x_i\right) \leq C\frac{N^{-2}\ln^2 N}{\sqrt{\varepsilon}}\varphi_i^n \quad \text{(by Lemma 10)}. \tag{32}$$

Considering the barrier functions

$$\psi_j^{\pm}(x_i) = C\left[N^{-2} + (N^{-2}\ln^2 N)\prod_{k=1}^{N}\left(1+h_k\sqrt{\frac{\beta}{\varepsilon}}\right)^{-1}\right]\varphi_i^j \pm (w-W)(x_i,t_j),$$

we observe that

$$\psi_j^{\pm}(x_0) \geq 0, \quad \psi_j^{\pm}(x_N) \geq 0,$$

and by Lemma 9,

$$\hat{\mathscr{K}}_\varepsilon^N \psi_j^{\pm}(x_i) \leq 0.$$

Applying the discrete minimum principle, the barrier functions satisfy $\psi_j^{\pm}(x_i) \geq 0$. Using the discrete barrier functions above and Lemma 7, we obtain

$$|(w-W)(x_i,t_j)| \leq CN^{-2}\ln^2 N.$$

Combining the errors for the regular and singular components yields the required result. □

Theorem 6. *The solution U_i^j of the fully discrete scheme (26) converges uniformly to the solution $u(x,t)$ of (2)and the error estimate is given by*

$$\sup_{0<\varepsilon\ll 1}\left|u(x_i,t_j) - U_i^j\right| \leq C(N^{-2}\ln^2 N + (\Delta t)^2), \quad i = 0,1,2,\ldots,N, \ \ j = 0,1,2,\ldots,M,$$

where C is constant independent of ε and the parameters N and Δt.

Proof. The proof is derived from the bounds established in Theorems 4 and 5. □

5 Numerical results and discussion

In this section, numerical results are presented in the form of tables and graphs to validate the theoretical findings. All computations are performed using the MATLAB R2015a programming language. For each ε the accuracy of the method is measured using maximum absolute errors. Since exact solutions for the model examples are unavailable, the maximum point-wise error is computed using the double mesh principle as follows:

$$e_\varepsilon^{N,M} = \max_{0\leq i,j\leq N,M}\left|U^{N,M}(x_i,t_j) - U^{2N,2M}(x_i,t_j)\right|$$

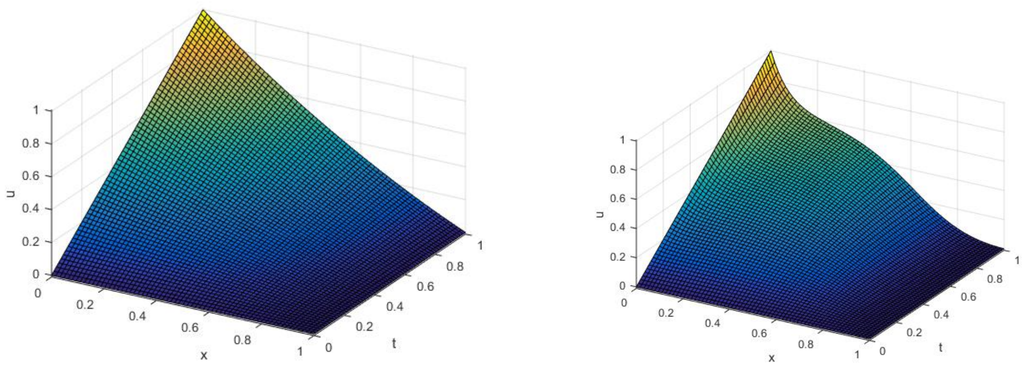

(a) $\varepsilon = 10^{-3}$ **(b)** $\varepsilon = 10^{-8}$

Figure 1: Surface plots of the numerical solution for Example 1 with $M = N = 64$ and $p = 2$.

and its corresponding numerical rate of convergence is

$$p_\varepsilon^{N,M} = \log_2(e_\varepsilon^{N,M}/e_\varepsilon^{2N,2M}).$$

Furthermore, $\varepsilon-$uniform point wise error is defined by

$$e^{N,M} = \max_\varepsilon e_\varepsilon^{N,M}$$

and its corresponding $\varepsilon-$uniform rate of convergence is

$$p^{N,M} = \log_2(e^{N,M}/e^{2N,2M}).$$

Example 1. Consider the problem in [37] as follows:

$$\begin{cases} \varepsilon u_{xx}(x,t) + x^p u_x(x,t) - u(x,t) - u_t(x,t) = x^2 - 1 + u(x,t-1)/2, & (x,t) \in \mathscr{W}. \\ u(0,t) = 1 + t^2, \;\; u(1,t) = 0, & 0 \le t \le 2, \\ u(x,t) = (1-x)^2, & \text{on } \; [0,1] \times [-1,0]. \end{cases}$$

Example 2. Consider the SPP in [37] as follows:

$$\begin{cases} \varepsilon u_{xx}(x,t) + x^p(1+te^{-2t})u_x(x,t) - (e^x+1)u(x,t) & \\ \qquad\qquad -u_t(x,t) = p(x^2-1)e^{-t} - tu(x,t-1), & (x,t) \in \mathscr{W}, \\ u(0,t) = 1 + t^2, \;\; u(1,t) = 0, & 0 \le t \le 2, \\ u(x,t) = (1-x)^2, & \text{on } \; [0,1] \times [-1,0]. \end{cases}$$

The maximum absolute errors and their corresponding rates of convergence for the proposed method, as demonstrated in Table 1 and Table 2, reveal that the method achieves second-order $\varepsilon-$uniform convergence. This is evidenced by the fact that the maximum absolute error remains constant for a fixed mesh parameter h as $\varepsilon \to 0$. Furthermore, as h decreases, the error decreases, indicating that the method is robust and accurate for a wide range of ε.

Table 1: Maximum absolute error and rate of convergence for Example 1 for $p = 1$.

$\varepsilon \downarrow M = N \rightarrow$	32	64	128	256	512
10^{-2}	5.8040e-04	1.6127e-04	4.0731e-05	1.0207e-05	2.5532e-06
	1.8476	1.9852	1.9966	1.9992	
10^{-8}	3.9221e-03	1.4052e-03	4.7519e-04	1.5488e-04	4.9010e-05
	1.4809	1.5642	1.6174	1.6600	
10^{-9}	3.9225e-03	1.4055e-03	4.7537e-04	1.5506e-04	4.9008e-05
	1.4808	1.5639	1.6163	1.6617	
10^{-10}	3.9227e-03	1.4055e-03	4.7541e-04	1.5509e-04	4.9038e-05
	1.4807	1.5639	1.6161	1.6611	
10^{-11}	3.9227e-03	1.4055e-03	4.7543e-04	1.5510e-04	4.9044e-05
	1.4807	1.5638	1.6161	1.6610	
10^{-12}	3.9227e-03	1.4056e-03	4.7543e-04	1.5510e-04	4.9045e-05
	1.4807	1.5638	1.6161	1.6610	
10^{-13}	3.9227e-03	1.4055e-03	4.7543e-04	1.5510e-04	4.9046e-05
	1.4807	1.5638	1.6161	1.6610	
$e^{M,N}$	3.9227e-03	1.4056e-03	4.7543e-04	1.5510e-04	4.9045e-05
$p^{M,N}$	1.4807	1.5638	1.6161	1.6610	
Method in [37]: $e^{M,N}$	4.308e-03	2.099e-03	1.055e-03	5.304e-03	2.741e-04
$p^{M,N}$	1.0373	0.9922	0.9923	0.9521	

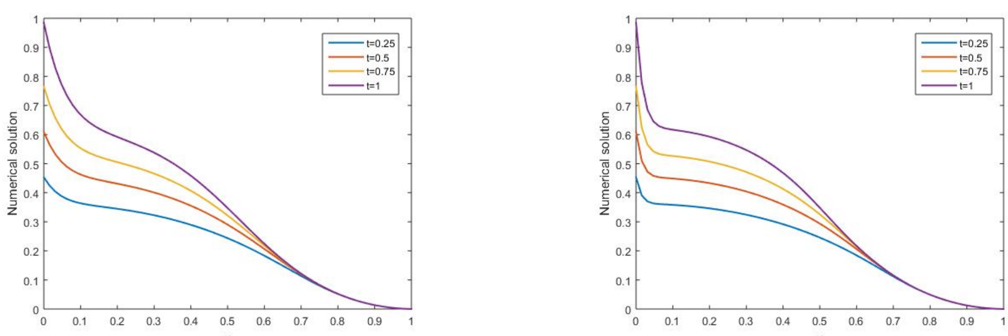

(a) $\varepsilon = 10^{-10},\ p = 1$ **(b)** $\varepsilon = 10^{-10},\ p = 3$

Figure 2: Surface plots of the numerical solution for Example 1 with $M = N = 64$ and different values of p.

Additionally, for various values of p with a fixed $\varepsilon = 10^{-13}$, the maximum errors and their corresponding orders of convergence are presented in Table 3. This table demonstrates that the variation in p has no impact on the stability or convergence of the method, highlighting its robustness across different parameter configurations.

Comparisons with other methods, as shown in Tables 1 and 2, demonstrate that the proposed method outperforms existing methods, such as the one in [37], in terms of both accuracy and order of convergence. This superior performance underscores the effectiveness of the proposed approach in solving singularly perturbed problems.

Table 2: Maximum absolute error and rate of convergence for Example 2 for $p = 1$.

$\varepsilon \downarrow M = N \rightarrow$	32	64	128	256	512
10^{-2}	5.2262e-03	1.3363e-03	3.3982e-04	8.5805e-05	2.1566e-05
	1.9675	1.9754	1.9856	1.9923	
10^{-8}	9.7632e-03	3.3025e-03	1.0779e-03	3.4669e-04	1.0846e-04
	1.5638	1.6153	1.6366	1.6765	
10^{-9}	9.7636e-03	3.3029e-03	1.0782e-03	3.4696e-04	1.0912e-04
	1.5637	1.6151	1.6358	1.6689	
10^{-10}	9.7637e-03	3.3030e-03	1.0783e-03	3.4700e-04	1.0916e-04
	1.5637	1.6150	1.6357	1.6685	
10^{-11}	9.7638e-03	3.3030e-03	1.0783e-03	3.4701e-04	1.0917e-04
	1.5637	1.6150	1.6357	1.6684	
10^{-12}	9.7638e-03	3.3030e-03	1.0783e-03	3.4701e-04	1.0917e-04
	1.5637	1.6150	1.6357	1.6684	
10^{-13}	9.7638e-03	3.3030e-03	1.0783e-03	3.4701e-04	1.0917e-04
	1.5637	1.6150	1.6357	1.6684	
$e^{M,N}$	9.7638e-03	3.3030e-03	1.0783e-03	3.4701e-04	1.0917e-04
$p^{M,N}$	1.5637	1.6150	1.6357	1.6684	
Method in [37]: $e^{M,N}$	1.965e-02	5.588e-03	1.950e-03	9.246e-04	4.475e-04
$p^{M,N}$	1.814	1.519	1.077	1.047	

Table 3: Maximum absolute error and its corresponding rate of convergence for $\varepsilon = 10^{-13}$ with different values of p.

$p \downarrow M = N \rightarrow$	32	64	128	256	512
	Example 1				
2	6.2464e-03	2.2696e-03	7.7517e-04	2.5337e-04	8.0196e-05
	1.4606	1.5499	1.6133	1.6596	
3	6.2464e-03	2.3077e-03	7.8566e-04	2.5500e-04	8.0196e-05
	1.4366	1.5545	1.6234	1.6689	
	Example 2		.	.	.
2	2.2137e-02	8.3890e-03	2.9063e-03	9.5685e-04	3.0327e-04
	1.3999	1.5293	1.6028	1.6577	
3	2.1922e-02	8.3114e-03	2.8822e-03	9.4839e-04	3.0060e-04
	1.3992	1.5280	1.6036	1.6577	

Surface plots in Figures 1 and 3 illustrate the formation of a left boundary layer in the solution. As $\varepsilon \rightarrow 0$, the boundary layer becomes thinner, and the proposed method effectively resolves it without requiring excessive mesh refinement. This capability is particularly important in singularly perturbed problems, where traditional methods often struggle to resolve boundary layers without significant computational effort. Furthermore, surface plots in Figures 2 and 4 demonstrate that as p increases, the peak of the solution becomes relatively increases and shifts away from the boundary layer region. The solu-

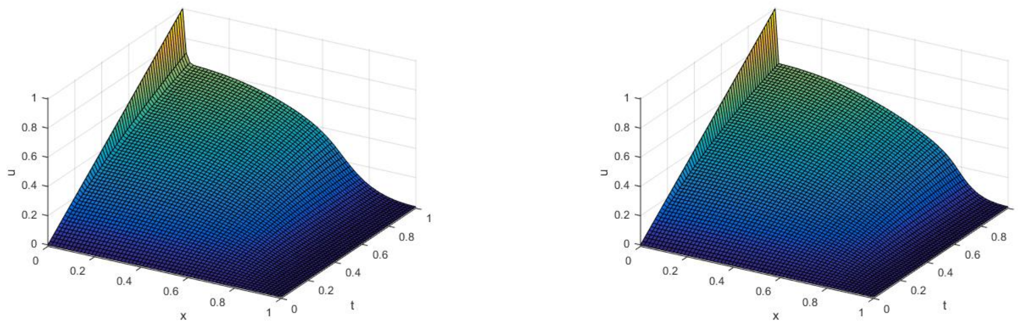

(a) $\varepsilon = 10^{-3}$ **(b)** $\varepsilon = 10^{-8}$

Figure 3: Surface plots of the numerical solution for Example 2 with $M = N = 64$ with $p = 1$.

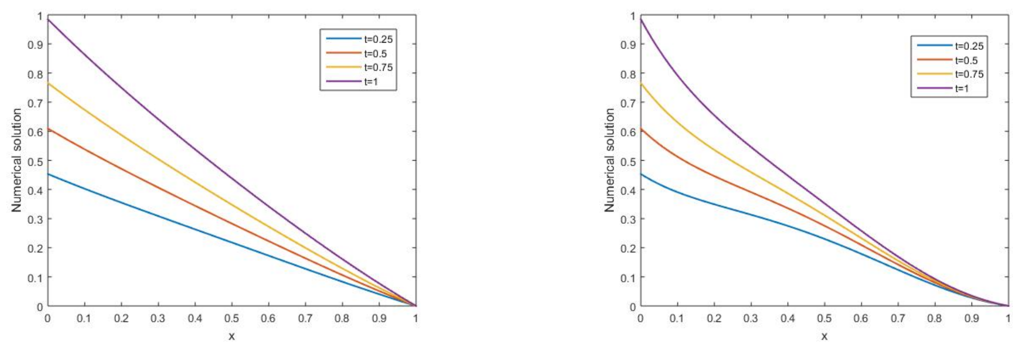

(a) $\varepsilon = 10^{-5},\ p = 2$ **(b)** $\varepsilon = 10^{-5},\ p = 3$

Figure 4: Surface plots of the numerical solution for Example 2 with $M = N = 64$ different values of p.

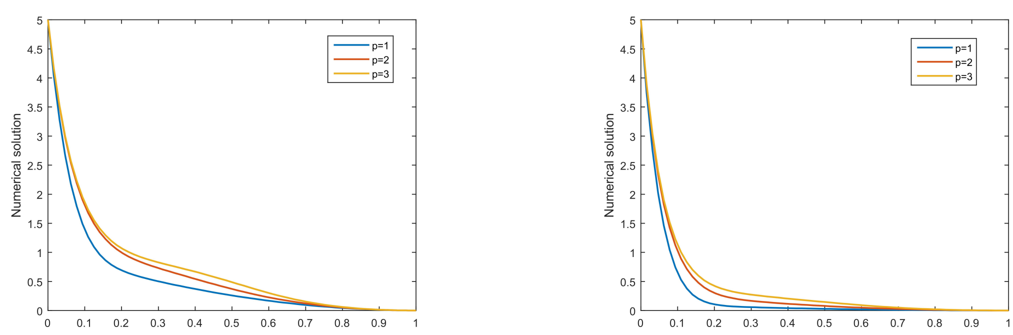

(a) Example 1 **(b)** Example 2

Figure 5: Solution profile for $\varepsilon = 10^{-2}$ with $M = N = 64$ and different values of p.

tion profile in Figure 5 for different p values strength this idea. This behavior highlights the interplay between the regular and boundary layer components of the solution, providing insight into the method's ability to handle complex solution structures.

6 Conclusion

In this paper, we considered time-delay singularly perturbed partial differential equations with multiple boundary turning points. The solution to this class of problems exhibits a left boundary layer in the spatial domain as the perturbation parameter approaches zero. The presence of the perturbation parameter, combined with the turning points, significantly complicates the problem, making it challenging to obtain an oscillation-free numerical solution. To address these difficulties, we developed a numerical scheme designed to solve such problems. The scheme employs the Crank-Nicolson method for time discretization on a uniform mesh and the central finite difference method for spatial discretization on a Shishkin mesh. The Shishkin mesh is particularly effective in resolving boundary layers and steep gradients, ensuring an accurate and stable numerical solution. The behaviour of the solution with respect to the perturbation parameter is illustrated using figures and tables, which visually demonstrate the effectiveness of the proposed scheme. These results confirm that the scheme is stable, achieves parameter-uniform convergence, and maintains almost second-order accuracy in both time and space. Numerical experiments conducted on model examples validate the theoretical findings, showing an agreement between the numerical solutions and the expected behavior. The proposed method is not only effective for the considered problems but also has the potential to be extended to solve more complex singularly perturbed delay parabolic turning point problems, such as those involving interior layers or higher dimensions. This adaptability makes the scheme a valuable tool for addressing a broader class of challenging problems in the field of singular perturbation theory.

Acknowledgements

The authors wish to appreciate the anonymous referees for their constructive suggestions which have helped to improve the manuscript notably.

References

[1] H.J. Al Salman, F.W. Gelu, A.A. Al Ghafli, *A fitted mesh robust numerical method and analysis for the singularly perturbed parabolic PDEs with a degenerate coefficient*, Results Appl. Math. **24** (2024) 100519.

[2] A.R. Ansari, S.A. Bakr, G.I. Shishkin, *A parameter-robust finite difference method for singularly perturbed delay parabolic partial differential equations*, J. Comput. Appl. Math. **205** (2007) 552–566.

[3] A. Das, L. Govindarao, J. Mohapatra, *A second order weighted monotone numerical scheme for time-delayed parabolic initial-boundary-value problem involving a small parameter*, Int. J. Math. Model. Numer. Optim. **12** (2022) 233–251.

[4] A. Das, S. Natesan, *Uniformly convergent hybrid numerical scheme for singularly perturbed delay parabolic convection–diffusion problems on Shishkin mesh*, Appl. Math. Comput. **271** (2015) 168–186.

[5] P. Deepika, A. Das, *A robust numerical scheme via grid equidistribution for singularly perturbed delay partial differential equations arising in control theory*, Int. J. Appl. Comput. Math. **10** (2024) 72.

[6] R.K. Dunne, E. O'Riordan, G.I. Shishkin, *A fitted mesh method for a class of singularly perturbed parabolic problems with a boundary turning point*, Comput. Methods Appl. Math. **3** (2003) 361–372.

[7] S. Elango, L. Govindarao, J. Mohapatra, R. Vadivel, N.T. Hu, *Numerical analysis for second-order differential equation of reaction-diffusion problems in viscoelasticity*, Alex. Eng. J. **92** (2024) 92–101.

[8] P. Farrell, A. Hegarty, J.M. Miller, E. O'Riordan, G.I. Shishkin, *Robust Computational Techniques for Boundary Layers*, Chapman and Hall/CRC, 2000.

[9] L. Govindarao, A. Das, *A second-order fractional step method for two-dimensional delay parabolic partial differential equations with a small parameter*, Palest. J. Math. **11** (2022) 96–111.

[10] L. Govindarao, J. Mohapatra, A. Das, *A fourth-order numerical scheme for singularly perturbed delay parabolic problem arising in population dynamics*, J. Appl. Math. Comput. **63** (2020) 171–195.

[11] T.C. Hanks, *Model relating heat-flow values near, and vertical velocities of mass transport beneath, oceanic rises*, J. Geophys. Res. **76** (1971) 537–544.

[12] A.F. Hegarty, J.J. Miller, E. O'Riordan, G. Shishkin, *Use of central-difference operators for solution of singularly perturbed problems*, Commun. Numer. Methods Eng. **10** (1994) 297–302.

[13] Y.M. Kebede, A.A. Tiruneh, E.G. Tsega, *Crank–Nicolson method for singularly perturbed unsteady parabolic problem with multiple boundary turning points*, Adv. Math. Phys. **2024** (2024) 4895771.

[14] Y.M. Kebede, A.A. Tiruneh, E.G. Tsega, *Fitted operator method for singularly perturbed delay parabolic problems with boundary turning points*, Int. J. Math. Math. Sci. **2025** (2025) 5581971.

[15] Y.M. Kebede, A.A. Tiruneh, E.G. Tsega, *Non-standard finite-difference scheme for singularly perturbed parabolic convection-diffusion problem with boundary turning points*, J. Math. Model. **2024** (2024) 85–103.

[16] R.B. Kellogg, A. Tsan, *Analysis of some difference approximations for a singular perturbation problem without turning points*, Math. Comput. **32** (1978) 1025–1039.

[17] P. Kumari, D. Kumar, H.R. Calle, *Parameter independent scheme for singularly perturbed problems including a boundary turning point of multiplicity greater than or equal to one*, J. Appl. Anal. Comput. **13** (2023) 1304–1320.

[18] H.G. Kumie, A.A. Tiruneh, G.A. Derese, F.A. Shah, *Crank–Nicolson method for solving time-fractional singularly perturbed delay partial differential equations*, Res. Math. **11** (2024) 2293373.

[19] T. Linß, M. Stynes, *Numerical methods on Shishkin meshes for linear convection–diffusion problems*, Comput. Methods Appl. Mech. Eng. **190** (2001) 3527–3542.

[20] A. Majumdar, S. Natesan, *An ε-uniform hybrid numerical scheme for a singularly perturbed degenerate parabolic convection-diffusion problem*, Int. J. Comput. Math. **96** (2019) 1313–1334.

[21] A. Majumdar, S. Natesan, *Second-order uniformly convergent Richardson extrapolation method for singularly perturbed degenerate parabolic partial differential equations*, Int. J. Appl. Comput. Math. **3** (2017) 31–53.

[22] W.G. Melesse, A.A. Tiruneh, G.A. Derese, *Uniform hybrid difference scheme for singularly perturbed differential-difference turning point problems exhibiting boundary layers*, Abstr. Appl. Anal. **2020** (2020) 7045756.

[23] W.G. Melesse, A.A. Tiruneh, G.A. Getachew, *Fitted mesh method for singularly perturbed delay differential turning point problems exhibiting twin boundary layers*, J. Appl. Math. Inform. **38** (2020) 113–132.

[24] J.J. Miller, E. O'Riordan, G.I. Shishkin, *Fitted Numerical Methods for Singular Perturbation Problems: Error Estimates in the Maximum Norm for Linear Problems in One and Two Dimensions*, World Sci., Singapore, 2012.

[25] J. Mohapatra, L. Govindarao, S. Priyadarshana, *A splitting-based higher-order numerical scheme for 2D time-dependent singularly perturbed reaction-diffusion problems*, J. Supercomput. **81** (2025) 203.

[26] J. Mohapatra, S. Priyadarshana, N.R. Reddy, *Uniformly convergent computational method for singularly perturbed time-delayed parabolic differential-difference equations*, Eng. Comput. **40** (2023) 694–717.

[27] M.J. Ng-Stynes, E. O'Riordan, M. Stynes, *Numerical methods for time-dependent convection-diffusion equations*, J. Comput. Appl. Math. **21** (1988) 289–310.

[28] S. Priyadarshana, *Monotone hybrid numerical method for singularly perturbed time-lagged semilinear parabolic problems*, Natl. Acad. Sci. Lett. **46** (2023) 347–350.

[29] S. Priyadarshana, J. Mohapatra, *An efficient computational technique for time dependent semilinear parabolic problems involving two small parameters*, J. Appl. Math. Comput. **69** (2023) 3721–3754.

[30] S. Priyadarshana, J. Mohapatra, *An efficient fractional step numerical algorithm for time-delayed singularly perturbed 2D convection-diffusion–reaction problem with two small parameters*, Numer. Algorithms **97** (2024) 687–726.

[31] S. Priyadarshana, J. Mohapatra, *Weighted variable-based numerical scheme for time-lagged semilinear parabolic problems including small parameter*, J. Appl. Math. Comput. **69** (2023) 2439–2463.

[32] S. Priyadarshana, J. Mohapatra, L. Govindarao, *An efficient uniformly convergent numerical scheme for singularly perturbed semilinear parabolic problems with large delay in time*, J. Appl. Math. Comput. **2022** (2022) 1–23.

[33] S. Priyadarshana, A. Padhan, J. Mohapatra, *Adaptive grid based moving mesh algorithms for singularly perturbed second-order Volterra integro-differential equations*, Quaest. Math. **2025** (2025) 1–22.

[34] S. Priyadarshana, J. Mohapatra, S.R. Pattanaik, *A second-order fractional step hybrid numerical algorithm for time-delayed singularly perturbed 2D convection-diffusion problems*, Appl. Numer. Math. **189** (2023) 107–129.

[35] S. Priyadarshana, J. Mohapatra, S.R. Pattanaik, *An improved time accurate numerical estimation for singularly perturbed semilinear parabolic differential equations with small space shifts and a large time lag*, Math. Comput. Simul. **214** (2023) 183–203.

[36] S. Priyadarshana, J. Mohapatra, H. Ramos, *Robust numerical schemes for time delayed singularly perturbed parabolic problems with discontinuous convection and source terms*, Calcolo **61** (2024) 1.

[37] P. Rai, S. Yadav, *Robust numerical schemes for singularly perturbed delay parabolic convection-diffusion problems with degenerate coefficient*, Int. J. Comput. Math. **98** (2021) 195–221.

[38] S.K. Sahoo, V. Gupta, *Second-order parameter-uniform finite difference scheme for singularly perturbed parabolic problem with a boundary turning point*, J. Differ. Equ. Appl. **27** (2021) 223–240.

[39] H. Schlichting, K. Gersten, *Boundary-Layer Theory*, Springer, New York, 2016.

[40] K.K. Sharma, P. Rai, K.C. Patidar, *A review on singularly perturbed differential equations with turning points and interior layers*, Appl. Math. Comput. **219** (2013) 10575–10609.

[41] J. Singh, S. Kumar, M. Kumar, *A domain decomposition method for solving singularly perturbed parabolic reaction-diffusion problems with time delay*, Numer. Methods Partial Differ. Equ. **34** (2018) 1849–1866.

[42] A.A. Tiruneh, G.A. Derese, D.M. Tefera, *A nonstandard fitted operator method for singularly perturbed parabolic reaction-diffusion problems with a large time delay*, Int. J. Math. Math. Sci. **2022** (2022) 5625049.

[43] M. Udupa, S. Saha, A. Das, *Computational analysis of blood flow through stenosed artery under the influence of body acceleration using Shishkin mesh*, Int. J. Appl. Comput. Math. **8** (2022) 107.

[44] S. Yadav, P. Rai, *A higher order scheme for singularly perturbed delay parabolic turning point problem*, Eng. Comput. **38** (2020) 819–851.

[45] S. Yadav, P. Rai, K.K. Sharma, *A higher order uniformly convergent method for singularly perturbed parabolic turning point problems*, Numer. Methods Partial Differ. Equ. **36** (2020) 342–368.